THE JOURNAL OF BIOLOGICAL CHEMISTRY VOL. 282, NO. 6, pp. 3951–3961, February 9, 2007

Structural and Functional Fingerprint of the Mitochondrial ATP-binding Cassette Transporter Mdl1 from *Saccharomyces cerevisiae*[*][S]

Received for publication, October 23, 2006, and in revised form, December 5, 2006 Published, JBC Papers in Press, December 6, 2006, DOI 10.1074/jbc.M609899200

Matthias Hofacker[‡], Simone Gompf[‡], Ariane Zutz[‡], Chiara Presenti[‡], Winfried Haase[§], Chris van der Does[‡1], Kirstin Model[§¶2], and Robert Tampé[‡3]

From the [‡]Institute of Biochemistry, Biocenter, Johann Wolfgang Goethe University, Max-von-Laue-Strasse 9, D-60438 Frankfurt am Main, Germany, [§]Structural Biology, Max Planck Institute of Biophysics, Max-von-Laue-Strasse 3, D-60438 Frankfurt am Main, Germany, and the [¶]MRC Laboratory of Molecular Biology, Hills Road, Cambridge CB2 2QH, United Kingdom

The ATP-binding cassette half-transporter Mdl1 from *Saccharomyces cerevisiae* has been proposed to be involved in the quality control of misassembled respiratory chain complexes by exporting degradation products generated by the m-AAA proteases from the matrix. Direct functional or structural data of the transport complex are, however, not known so far. After screening expression in various hosts, Mdl1 was overexpressed 100-fold to 1% of total mitochondrial membrane protein in *S. cerevisiae*. Based on detergent screens, Mdl1 was solubilized and purified to homogeneity. Mdl1 showed a high binding affinity for MgATP (K_d = 0.26 μM) and an ATPase activity with a K_m of 0.86 mM (Hill coefficient of 0.98) and a turnover rate of 2.6 ATP/s. Mutagenesis of the conserved glutamate downstream of the Walker B motif (E599Q) or the conserved histidine of the H-loop (H631A) abolished ATP hydrolysis, whereas ATP binding was not affected. Mdl1 reconstituted into liposomes showed an ATPase activity similar to the solubilized complex. By single particle electron microscopy, a first three-dimensional structure of the mitochondrial ATP-binding cassette transporter was derived at 2.3-nm resolution, revealing a homodimeric complex in an open conformation.

The ATP-binding cassette (ABC)[4] superfamily constitutes a large class of active transporters found in all kingdoms of life. They couple the hydrolysis of ATP to the transport of substrates across membranes. ABC transporters are composed of two transmembrane domains (TMDs) and two nucleotide-binding domains (NBDs). The TMDs form the translocation pore, whereas the NBDs are responsible for ATP binding and ATP hydrolysis, thus energizing substrate transport (1, 2). In prokaryotes and archaea, they can function as importers together with a substrate-binding protein, but generally ABC transporters operate as exporters. The TMDs and NBDs are found as homo- or heterodimers and can be arranged in any combination, *e.g.* as separate polypeptides, as single polypeptides, or as half-size transporters with fused TMD and NBD. The NBDs contain the highly conserved Walker A and B motifs as well as the C-, H-, and D-loops. Structural and biochemical data demonstrated that ATP binding induces dimerization of two NBDs in a head-to-tail orientation leading to a structure where both ATPs are sandwiched on the interface of the dimer (reviewed in Ref. 3). Each of the two nucleotide-binding sites in the dimer is formed by the Walker A and B motifs from one NBD and C-loop residues of the other NBD.

The *MDL1* gene encodes a membrane protein of 695 amino acids with a TMD followed by a NBD (4). Hydrophobicity and sequence homology analysis suggested that the TMD contains six transmembrane helices with the N and C termini located in the matrix. The minimal functional unit has been suggested to be a homodimer residing in the inner mitochondrial membrane (5). Mdl1 is a component of the mitochondrial quality control system and is involved in translocation of peptides with a length of 6–20 amino acids from the matrix into the inter membrane space (5). These products are generated by degradation of non-assembled inner mitochondrial membrane complexes by m-AAA (matrix-oriented ATPases associated with a variety of cellular activities) proteases (6). Although Mdl1 is not essential for cell viability, it is tempting to speculate that it plays a physiological role in the communication between the mitochondrion and the cellular environment. Homologues of Mdl1 have been identified in mammals, *e.g.* ABCB8 (M-ABC1) and ABCB10 (ABC-me, M-ABC2) (7–9). Several other functions for Mdl1 have, however, been suggested, *e.g.* Mdl1 partially restores Atm1 function (10). The ABC transporter Atm1 serves as a link between mitochondrial and cytosolic iron homeostasis, presumably by exporting iron-sulfur clusters assembled in the mitochondrial matrix into the intermembrane space (11). Overexpression of Mdl1 in Δ*atm1* cells results in a reduction of mitochondrial iron content and decreased sensitivity to H_2O_2 and transition metal toxicity, thus suggesting a role for Mdl1 in the regulation of cellular resistance to oxidative stress.

Here, we report the overexpression, purification, and functional reconstitution into proteoliposomes of Mdl1, which

* This work was supported by the Deutsche Forschungsgemeinschaft. The costs of publication of this article were defrayed in part by the payment of page charges. This article must therefore be hereby marked "*advertisement*" in accordance with 18 U.S.C. Section 1734 solely to indicate this fact.
[S] The on-line version of this article (available at http://www.jbc.org) contains supplemental Tables S1 and S2.
[1] Supported by a TALENT fellowship of the Netherlands Organization for scientific research (NWO).
[2] Supported by European Union Grant LSHG-CT-2004-005257.
[3] To whom correspondence should be addressed. Tel.: 49-69-798-29475; Fax: 49-69-798-29495; E-mail: tampe@em.uni-frankfurt.de.
[4] The abbreviations used are: ABC, ATP-binding cassette; DDM, *n*-dodecyl-β-D-maltoside; EM, electron microscopy; FC-14, tetradecylphosphocholine; NBD, nucleotide-binding domain; TMD, transmembrane domain.

allowed us to study the biochemical properties of a mitochondrial ABC transporter for the first time. In addition, the three-dimensional structure of the ABC transport complex was obtained at 2.3-nm resolution by electron microscopy and single particle analysis.

EXPERIMENTAL PROCEDURES

Materials— 8-Azido-[α-^{32}P]ATP was purchased from MP Biomedicals. Peptide libraries were synthesized by Fmoc (*N*-(9-fluorenyl)methoxycarbonyl) solid phase chemistry (12). For immune detection, rabbit antisera were raised against the C terminus of Mdl1 (KGGVIDLDNSVAREV) and affinity-purified. Protein concentrations were determined using the Bradford assay (Pierce). Digitonin was purchased at Calbiochem, and all other detergents were from Anatrace.

Cloning—By the use of unique restriction sites, *MDL1* was systematically divided in three cassettes, facilitating exchange between different constructs. The cassettes were amplified by PCR from genomic DNA. Cassette I encodes the N terminus of Mdl1 until a silent ClaI site, which was introduced at the nucleotides corresponding to residue S221. Cassette II includes the central region of Mdl1 from the ClaI site to an intrinsic and unique BamHI site comprising amino acids Ser^{221}–Lys^{422}. Cassette III encodes the NBD from amino acid Asp^{423} to the C terminus including an additional His$_8$ tag. A variant of cassette III was cloned without a C-terminal tag and named IIIa. Cassette I was also constructed without the first 68 amino acids, predicted to include the mitochondrial leader sequence, and named Ia. Primers used to generate the cassettes are described in the on-line supplemental material (supplemental Table S1). The cassettes I, II, and III were sequentially ligated into pET401 (13) resulting in vector pMDL1(pre).

Construction of Expression Plasmids—The *MDL1* gene from vector pMDL1(pre) was cloned in different cloning and expression vectors for either *Escherichia coli* or *Lactococcus lactis* (supplemental Table S2). To integrate the *MDL1* gene behind the strong *PDR5* promotor, a PCR fragment was created by using pMDL1(pre) as template as well as the pc4(f) and pc4(r) primers. The resulting PCR fragment was digested with AscI and PacI and ligated into pFA6a-His3MX6 (14). This vector was used as a template to generate a PCR fragment with the primers pc5(f) and pc5(r), which was then used for homologous recombination in the *Saccharomyces cerevisiae* strain YALF-A1 (15). To generate the yeast overexpression vector, the *MDL1* gene from vector pMDL1(pre) was amplified by PCR using the primers pc6(f) and pc3(r) and cloned into pYES2.1/V5-His-TOPO (Invitrogen) via the TOPO TA Expression kit (Invitrogen). This resulted in a galactose-inducible Mdl1 construct with a C-terminal 4-Gly spacer, a factor X$_a$ cleavage site and an His$_8$ tag.

Expression in E. coli and L. lactis—The *E. coli* expression plasmids were transformed into different *E. coli* strains, *e.g.* BL21(DE3) (Novagen), C41 (16), C43 (16), SF100 (17), and TOP10 (Invitrogen). The strains were grown in LB medium at different temperatures (18, 25, 30, and 37 °C). Depending on the respective system, the expression was induced by the addition of isopropyl β-D-thiogalactopyranoside (0.025, 0.1, 0.2, and 0.5 mM) or arabinose (0.004, 0.04, and 0.4%) at different A_{600} (0.2, 0.6, and 1.0) for different times (1, 2, 3, and 6 h and overnight). The different plasmids were co-transformed into strains containing plasmids encoding for rare tRNAs (pRARE). To assist membrane insertion, the *MDL1* gene cloned into pK184 (18) was co-expressed with the SecY, SecE, SecG, and YidC components of the *E. coli* translocase (19). For expression in *L. lactis*, strain NZ9000 (20) was transformed with pNZ8084-Mdl1fl. The expression was tested under conditions where extra chaperones were produced, *e.g.* in the presence of 1 M sorbitol, 2% ethanol, or at 42 °C. The membranes were isolated as described (21) and separated on SDS-PAGE (10%), and the expression levels were evaluated by quantitative immunoblotting and immunodetection using an anti-Mdl1 antibody. Purified Mdl1-NBD was used as reference (22), and quantification was carried out with a Lumi-Imager F1 (Roche Applied Science) and the LumiAnalyst software (version 3.1).

Overexpression in S. cerevisiae—*S. cerevisiae* strain BY4743 (MATa/MATα; his3Δ1/his3Δ1; leu2Δ0/leu2Δ0; met15Δ0/MET15; LYS2/lys2Δ0; ura3Δ0/ura3Δ0) (23) was transformed with the plasmid pYES2.1/V5-His-TOPO-Mdl1fl, pYES2.1/V5-His-TOPO-Mdl1fl_EQ, or pYES2.1/V5-His-TOPO-Mdl1fl_HA and grown overnight in SC medium (24), supplemented with amino acids without uracil and 2% glucose. The cells were harvested and resuspended to an A_{600} of 0.4 in SC medium supplemented with amino acids without uracil and 2% galactose. Growth was continued at 30 °C, and cells were harvested by centrifugation 8 h after induction. The mitochondria were isolated as described (25). The proteins were separated on SDS-PAGE (10%), and the expression levels were evaluated by Coomassie staining and quantitative immunoblotting.

Detergent Screens—To test the solubilization efficiencies, the mitochondria (5 mg/ml) were solubilized for 30 min in 100 μl of buffer S (50 mM Tris-HCl, 150 mM NaCl, 15% (v/v) glycerol, 2 mM imidazole, pH 7.5) supplemented with DDM, FC-14, or digitonin at ρ values of either 15 or 50 (Equation 1; where [lipid] is 0.1 times (w/w) the protein concentration, the average molecular mass of a lipid was taken as 875 Da, and *CMC* is the critical micelle concentration).

$$\rho = \frac{[\text{detergent}] - CMC}{[\text{lipid}]} \qquad \text{(Eq. 1)}$$

After ultracentrifugation (100,000 × *g*, 30 min, 4 °C), solubilized and nonsolubilized Mdl1 were compared by immunoblotting using an Mdl1-specific antibody. Chemiluminescent signals were quantified, and the percentage of solubilized protein was calculated. To analyze the stability and oligomeric state of Mdl1 mitochondria (0.5 mg of protein in 100 μl of final volume) were solubilized in different detergents (1% each). Solubilized proteins were separated by ultracentrifugation (100,000 × *g*, 30 min, 4 °C) and analyzed by Blue native electrophoresis (gradient 6.0 to 16.5%) as described (26). Thyroglobulin (669 kDa), ferritin (440 kDa), catalase (232 kDa), and lactate dehydrogenase (140 kDa) were used as markers.

Purification of Mdl1—Mitochondria (5 mg/ml) were solubilized in buffer S supplemented with 1% digitonin (ρ value of 15) and EDTA-free complete protease inhibitor mixture (Roche Applied Science) for 30 min at 4 °C under gentle shaking. Sol-

uble and insoluble fractions were separated by ultracentrifugation (100,000 × *g*, 30 min, 4 °C), and the supernatant was applied to an IDA-column (GE Healthcare) loaded with Ni^{2+} and equilibrated with IMAC buffer (50 mM Tris-HCl, 150 mM NaCl, 15% (v/v) glycerol, 2 mM imidazole, 0.1% digitonin, pH 7.5). The column was washed with 60 and 120 mM imidazole. Specifically bound protein was eluted in IMAC buffer containing 200 mM imidazole. The protein was identified by immunoblotting and matrix-assisted laser desorption/ionization time-of-flight peptide mass fingerprint analysis after trypsin digestion, using Mascot (data base NCBInr 20040521).

Nucleotide Binding Assays—Nucleotide binding was measured by 8-azido-[α-^{32}P]ATP photo cross-linking experiments. Purified Mdl1 (0.5 μM) was incubated with increasing concentrations of 8-azido-[α-^{32}P]ATP for 5 min on ice and UV-irradiated for 5 min. For concentrations of 10 μM and above, 8-azido-[α-^{32}P]ATP was supplemented 1:5 with nonradioactive 8-azido-ATP. Subsequently, samples were analyzed by SDS-PAGE (10%). The gels were dried and exposed to a Kodak SO230 phosphor screen. Photo cross-linked protein was quantified by phosphorimaging (Phosphor-Imager 445Si, Molecular Dynamics). Intensities (*I*) were plotted against the 8-azido-ATP concentration and fitted with a (1:1) Langmuir isotherm. To determine the half-maximal inhibitory concentration (IC_{50}) for MgATP, Equation 2 was used (where *bg* displays background intensity).

$$I = \frac{I_{max}}{1 + \left(\frac{[\text{8-azido-ATP}]}{IC_{50}}\right)^{\text{slope}}} + bg \qquad \text{(Eq. 2)}$$

Applying the Cheng-Prusoff equation (27), the dissociation constant K_d for ATP was derived from the IC_{50} value for ATP and the K_d value for 8-azido-ATP (Equation 3).

$$K_{d(\text{ATP})} = \frac{IC_{50}}{1 + \frac{[\text{8-azido-ATP}]}{K_{d(\text{8-azido-ATP})}}} \qquad \text{(Eq. 3)}$$

ATP Hydrolysis Assay—The ATPase activity was determined essentially as described (28). Briefly, 25 μl of ATP buffer (50 mM Tris-HCl, 150 mM NaCl, 20 mM $MgCl_2$, pH 7.5) with varying concentrations of ATP supplemented with [γ-^{32}P]ATP (4 μCi; Hartmann Analytic) and 0.02% (w/v) FC-14, 0.02% (w/v) DDM or 0.1% (w/v) digitonin was mixed with 25 μl of purified Mdl1 (final concentration, 0.5 μM) and incubated for 10 min at 30 °C. The reaction was stopped by the addition of 1 ml of reagent A (10 mM ammonium molybdate in 1 N HCl), 15 μl of 20 mM H_3PO_4, and 2 ml of reagent B (isobutanol, cyclohexane, acetone, and reagent A in a ratio of 5:5:1:0.1). The mixture was vortexed vigorously for 30 s. After phase separation, 1 ml of the organic phase was mixed with scintillation fluid (Microscint; Packard BioScience), and the release of inorganic phosphate was determined by β-counting (Beckman LS 6500 liquid scintillation counter). V_{max} and K_m were derived by fitting the data to the Michaelis-Menten equation. A similar protocol was used to determine the ATPase activity of reconstituted Mdl1.

Reconstitution of Mdl1—E. coli total lipids (Avanti Polar Lipids) were resuspended in buffer R (50 mM Tris, 25 mM KCl, pH 7.5) at a concentration of 4 mg/ml. The lipid suspension was extruded (Avanti Mini-Extruder) 11 times through a 0.4-μm polycarbonate filter (Avestin). The liposome suspension was titrated to a final DDM concentration of 4.2 mM, mixed with solubilized Mdl1 in a molar lipid-to-protein ratio of 200, and incubated for 30 min at 20 °C. Polystyrene beads (Bio-beads SM-2; Bio-Rad) were washed three times with methanol, washed five times with buffer R, and incubated with *E. coli* total lipids (4 mg/ml in buffer R) before use. These Bio-beads (80 mg/ml final) were then added to the protein/detergent/lipid mixture and incubated overnight at 4 °C. Bio-beads were replaced by freshly prepared beads (80 mg/ml) and incubated for 1 h at 4 °C. After removal of the Bio-beads, proteoliposomes were pelleted by ultracentrifugation (190,000 × *g*, 1 h, 4 °C), resuspended in buffer R, applied to a sucrose step gradient (10, 20, and 30% (w/v)), and centrifuged (100,000 × *g*, 18 h, 4 °C). The sucrose concentration of each fraction was determined with an Abbé refractometer. The lipid concentration was determined as described (29). Briefly, 100-μl samples were mixed with the same volume of 70% (v/v) perchloric acid, and after incubation for two hours at 200 °C, 700 μl of reagent C (2.5% (w/v) ammonium molybdate, 12.5% perchloric acid) and 700 μl of 3% (w/v) ascorbic acid were added. Finally, the samples were incubated for 5 min at 100 °C, and absorbance at 820 nm was measured and compared with a phosphate standard (Sigma-Aldrich). The protein concentration in the different fractions was determined by quantitative immunoblotting using isolated Mdl1 as a reference. To elucidate the orientation of reconstituted Mdl1, proteoliposomes were treated with the protease factor X_a at 10 μg/ml for 2 h at 25 °C in the presence of 1 mM $CaCl_2$.

Freeze Fracture Electron Microscopy—Proteoliposome preparations were placed between two small copper blades and rapidly frozen in liquid ethane. The samples were prepared in a freeze fracture unit (400T Balzers) and shadowed with platinum/carbon at an angle of 45°. Replicas reinforced by pure carbon shadowing at an angle of 90° were cleaned from organic material in chromo-sulfuric acid and analyzed by a Philips EM208S electron microscope.

Peptide Transport Assays—Iodination of peptide libraries and peptide transport was performed as described (30). Proteoliposomes (0.5 μg of Mdl1) were preincubated with 4.8 mM ATP and 10 mM $MgCl_2$ in 50 μl of transport buffer (50 mM Tris, 25 mM KCl, 0.1 mM dithiothreitol, pH 7.5) for 1 min at 30 °C. The transport reaction was started by the addition of ^{125}I-labeled X_8 or X_{23} peptide libraries to a final concentration of 2 μM. The reaction was stopped after 6 min at 30 °C by the addition of 500 μl of ice-cold transport buffer supplemented with 10 mM EDTA. After centrifugation, the pellets were washed, and radioactivity was quantified by γ-counting. To determine background activities, the samples were treated with apyrase (1 unit) instead of MgATP.

Single Particle Electron Microscopy—Purified Mdl1(H631A) was concentrated (Amicon Ultra-4; molecular weight cut-off 100 kDa) to 1 mg/ml, subjected to gel filtration (Superdex 200 PC 3.2), and equilibrated with buffer G (50 mM Tris-HCl, 150 mM NaCl, 0.1% digitonin, pH 7.5). Peak fractions containing

Mdl1 were pooled, applied on a carbon grid, and stained with 2% uranyl acetate.

Electron microscopy (EM) images were recorded on film under low dose conditions in a FEI F30 electron microscope. For three-dimensional reconstruction, tilt pairs were collected at 0° and 48° tilt and corresponding micrographs digitized on a Zeiss SCAI Scanner with 7-μm pixel size. Particle images were analyzed using the SPIDER package (31). XMIPP software (32) was used for classification of untilted images based on the Kohonen neural network. The maps were obtained from a total data set of 2 × 1404 projections by the random conical tilt method (33). The 2-fold symmetry typical for homodimers was imposed after verification at the latest step. After multiple refinements of all three Euler angles, the final volume was computed. The resolution was determined by the Fourier shell correlation criterion (cut-off at five times the noise correlation, FSC_5). The atomic structure of the open MsbA (Protein Data Bank code 1JSQ (34)) was fitted into the electron density map of Mdl1 using Chimera software (35).

TABLE 1
Expression level of Mdl1 in various hosts

	S. cerevisiae wild type[a]	Plasmid-driven expression		
		E. coli	*L. lactis*	*S. cerevisiae*[a]
	%		%	
Amount/total membrane protein (*w*/*w*)	0.01	0.005	0.01	1

[a] Mitochondrial membranes.

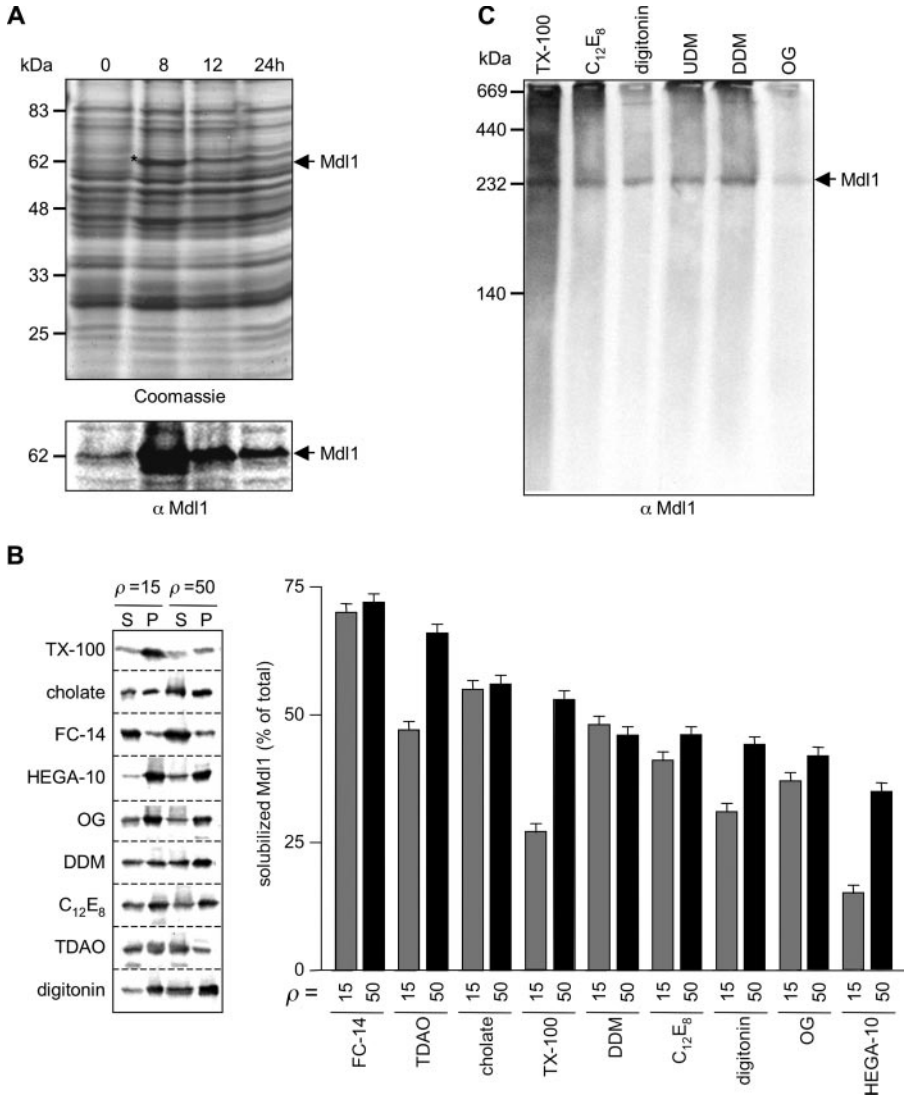

FIGURE 1. **Expression, solubilization, stability, and oligomeric state of Mdl1.** *A*, mitochondria isolated at different time points after induction were analyzed by SDS-PAGE (10%) followed by Coomassie staining (*upper panel*) and immunoblotting (*lower panel*). 15 μg of protein were applied per lane. This shows that Mdl1 was overexpressed 8 h after induction (*). *B*, mitochondria (0.5 mg of total protein) were resuspended in 100 μl of buffer S supplemented with different detergents as indicated (ρ values of 15 or 50). Solubilized (*S*) and non-solubilized proteins (pellet, *P*) were separated by ultracentrifugation (100,000 × *g*) and analyzed by SDS-PAGE (10%). Mdl1 was detected by immunoblotting (*left panel*). The *right panel* depicts a quantification of the data. *C*, mitochondria (0.5 mg in 100 μl) were solubilized in detergents (1% each) as indicated. The details are given under "Experimental Procedures." Solubilized proteins were separated by ultracentrifugation (100,000 × *g*) and analyzed by Blue native electrophoresis and immunoblotting. Thyroglobulin (669 kDa), ferritin (440 kDa), catalase (232 kDa), and lactate dehydrogenase (140 kDa) were used as markers. $C_{12}E_8$, octaethylene glycol monododecyl ether; *HEGA-10*, *n*-decanoyl-*N*-hydroxyethylenglucamide; *OG*, *n*-octyl-α-D-glucopyranoside; *TDAO*, *n*-tetradecyl-*N*,*N*-dimethylamine-N-oxide; *UDM*, *n*-undecyl-β-D-maltoside; *TX-100*, Triton X-100.

RESULTS

To collect the first biochemical and structural data of a mitochondrial ABC transporter, we set out to screen optimal conditions for expression, solubilization, purification, and reconstitution of Mdl1. In *S. cerevisiae*, Mdl1 is expressed at low levels (36) and is almost unaffected by various stimuli (environmental stress) as shown by microarray techniques (db.yeastgenome.org). Quantitative immunoblotting using the isolated NBD of Mdl1 as reference (22) demonstrated that Mdl1 is expressed to approximately 0.01% (w/w) of total mitochondrial protein (Table 1). We first tested expression of Mdl1 in *E. coli*. High and low copy number plasmids with different inducible promotors were studied under varying growth conditions and in different strains. The expression level of Mdl1 was determined by quantitative immunoblotting as described above. To promote Mdl1 expression, chaperones were induced by growth at 42 °C either in the presence of 2% ethanol or 1 M sorbitol. In addition, we tested co-expression with rare tRNAs or the SecY, SecE, SecG, and YidC components of the *E. coli* translocase. However, none of these factors improved the expression level of Mdl1 (0.005% of total membrane protein; Table 1). Because *L. lactis* has been demonstrated to be a suitable host for overexpression of mitochondrial proteins (37), Mdl1

was also expressed in this *gram*-positive bacteria. Expression of Mdl1 under control of a strong, nisin-inducible promotor led to an ~2-fold higher expression level (0.01% of total membrane protein) compared with *E. coli*, but the expression level was still very low (Table 1).

Because only low expression levels were obtained in either *E. coli* or *L. lactis*, we initiated expression screens in *S. cerevisiae*. MDL1 was cloned behind a strong constitutive glyceraldehyde-3-phosphate dehydrogenase promotor ($p426^{GPD}$) or strong glycerol-dependent AAC2 (ADP/ATP carrier protein) promotor ($pYES3P_{A2}AAC2$). Surprisingly, both approaches resulted in lower than intrinsic levels of Mdl1 (Table 1). Alternatively, *Mdl1* was cloned behind the *PDR5* promotor, which is under control of the *PDR* network in the *S. cerevisiae* strain YALF-A1 (15). This system has been successful in the expression of membrane proteins in yeast (38–40). However, also in this case, only reduced levels of Mdl1 were obtained. We next examined expression from a multicopy plasmid under the inducible *GAL1* promotor. Here, Mdl1 was overexpressed 100-fold, reaching 1% of total mitochondrial protein (Table 1). Mdl1 expression was strongly time-dependent, reaching its maximum 8 h after induction and then decreasing (Fig. 1*A*). This finding indicates that high Mdl1 levels are disfavored and result in increased instability or degradation of the protein. The degradation pathway is presently not known and is the focus of future studies. However, using this expression system, high levels of Mdl1 suitable for functional and structural studies were obtained.

We subsequently tested various detergents at different concentrations (ρ value) for optimal solubilization of Mdl1 from isolated mitochondria. *n*-Tetradecylphosphocholine (FC-14) showed by far the highest solubilization efficiency (>70% at ρ = 50) followed by *n*-tetradecyl-*N*,*N*-dimethylamine-*N*-oxide (66%), sodium cholate (56%), Triton X-100 (53%), and finally DDM (48%), octaethylene glycol monododecyl ether (46%), digitonin (44%), *n*-octyl-α-D-glucopyranoside (42%), and *n*-decanoyl-*N*-hydroxy ethylenglucamide (35%) (Fig. 1*B*). We then investigated the stability and oligomeric state of Mdl1 in different detergents by Blue native electrophoresis (Fig. 1*C*). Mdl1 migrated as a defined band at 250 kDa in Triton X-100, octaethylene glycol monododecyl ether, digitonin, *n*-undecyl-β-D-maltoside, DDM, and *n*-octyl-α-D-glucopyranoside. In case of digitonin, Mdl1 was found in an almost monodisperse state corresponding to a homodimeric complex. Only a very broad smear was observed if Mdl1 was solubilized in FC-14 (not shown).

Mdl1 was isolated by metal affinity chromatography utilizing a C-terminal His_8 tag. Purification was analyzed by SDS-PAGE and immunoblotting (Fig. 2*A*). Like many integral membrane proteins, Mdl1 migrates at lower molecular mass than predicted (62 kDa instead of 71 kDa). Mdl1 was further identified by peptide mass fingerprinting. Three detergents were selected for further analysis: FC-14 as the most efficient detergent for solubilization, DDM known to preserve active ABC transporters and often used in crystallization of membrane proteins (41), and digitonin reported to hold fragile membrane protein complexes together (42). 1 mg of FC-14-solubilized Mdl1 (>95% purity) was isolated from 6 liters of yeast culture, 0.2 mg in case

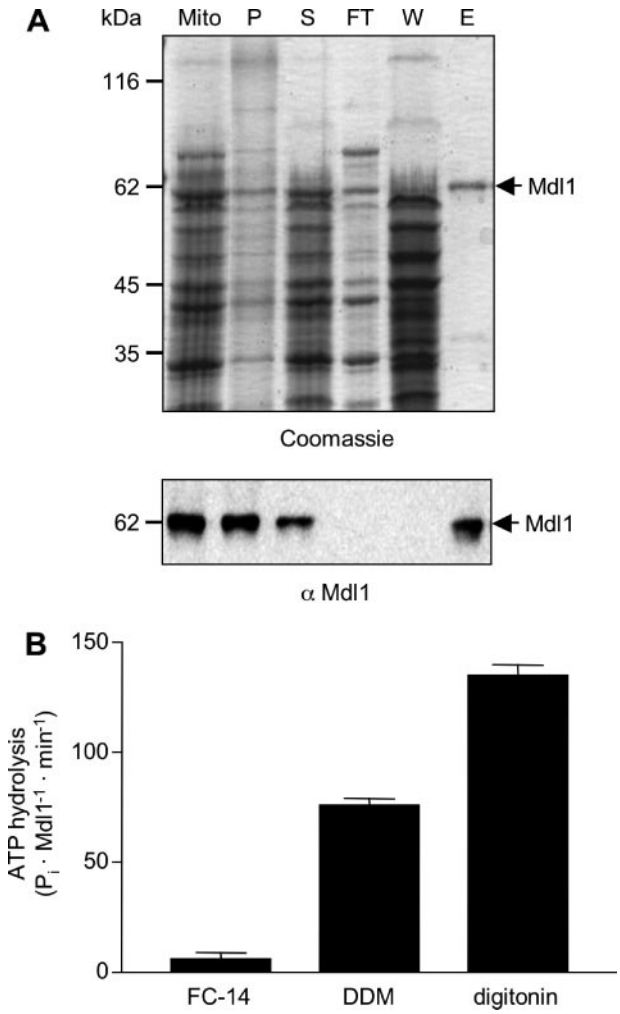

FIGURE 2. **Purification and ATPase activity of Mdl1 in different detergents.** *A*, solubilization and purification of His_8-tagged Mdl1 via metal affinity chromatography. Mitochondria (*Mito*), pellet (*P*) and supernatant (*S*) after solubilization with 1% digitonin, flow through (*FT*), wash fraction at 60 mM imidazole (*W*), elution with 200 mM imidazole (*E*) are depicted. The protein band at 62 kDa was identified as Mdl1 by immunoblotting using Mdl1-specific antibodies (*lower panel*) and peptide mass fingerprinting. *B*, ATPase activity of Mdl1 (0.5 μM) purified in different detergents. Mitochondria (5 mg/ml) overexpressing Mdl1 were solubilized in FC-14, DDM, or digitonin (1% each) and purified as described under "Experimental Procedures" (concentration of FC-14 was 0.01%, 0.02% for DDM, and 0.01% for digitonin). ATP hydrolysis was measured at 30 °C immediately after purification in the presence of 5 mM ATP.

of DDM and 0.1 mg for digitonin. For each detergent, the ATPase activity of purified Mdl1 was determined, and remarkable differences were observed (Fig. 2*B*). Based on its high ATPase activity and almost monodisperse state, Mdl1 solubilized and purified in the presence of digitonin was selected for further functional and structural analysis.

To examine the nucleotide binding properties of Mdl1, 8-azido-[α-^{32}P]ATP photo cross-linking experiments were performed. The apparent affinity constant for 8-azido-ATP was determined to be 7 μM according to a Langmuir-type (1:1) binding curve (Fig. 3*A*). Photo cross-linking of Mdl1 by 8-azido-[α-^{32}P]ATP (5 μM) was inhibited by MgATP with an IC_{50} value of 0.45 μM (Fig. 3*B*). Based on the apparent affinity of 8-azido-ATP, a dissociation constant for MgATP of 0.26 μM was estimated. ADP, CTP, UTP, and GTP show a similar affinity pat-

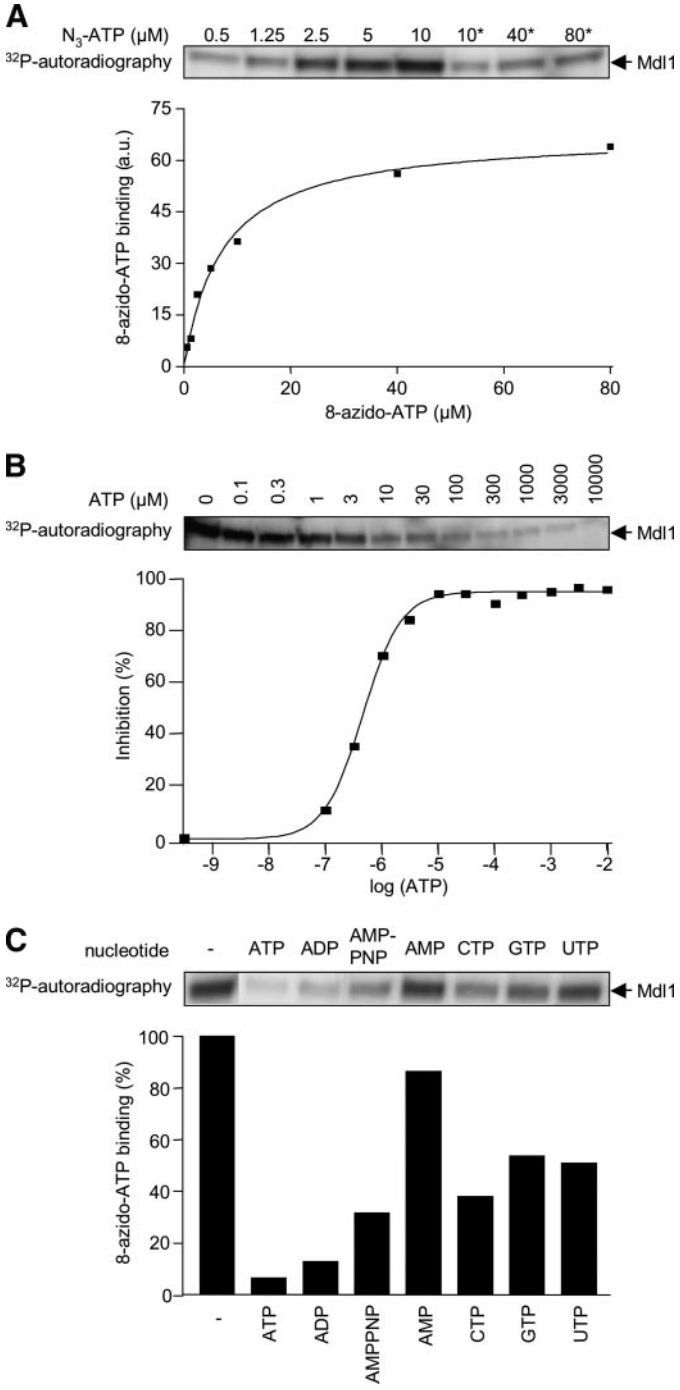

FIGURE 3. **Nucleotide binding properties of Mdl1.** Digitonin-solubilized Mdl1 (0.5 μM) was incubated with 8-azido-[α-^{32}P]ATP for 5 min on ice, and photo cross-linking was performed as described under "Experimental Procedures." The same amount of protein was applied in each lane. *A*, 8-azido-[α-^{32}P]ATP photo cross-linking. For high concentrations (10 μM and above, indicated by *asterisks*), 8-azido-[α-^{32}P]ATP was supplemented with nonradioactive 8-azido-ATP (1:5). The intensities of substituted 8-azido-[α-^{32}P]ATP were adjusted to the nonsubstituted sample by comparing the intensities at 10 μM. The photo cross-linking efficiencies were quantified by phosphorimaging and plotted against the concentration of 8-azido-ATP. The data were fitted by a Langmuir isotherm (1:1) resulting in an apparent dissociation constant of 7 μM. *B*, ATP competition of 8-azido-ATP photo cross-linking. Photo cross-linking was performed with 5 μM of 8-azido-[α-^{32}P]ATP with increasing concentrations of MgATP. The intensities were plotted against the ATP concentration and fitted to Equation 3, leading to an IC_{50} value of 0.45 μM. *C*, nucleotide binding specificity of Mdl1. Photo cross-linking was performed with 5 μM of 8-azido-[α-^{32}P]ATP in the presence of various nucleotides (0.3 mM each). The sample without competitor was set to 100%.

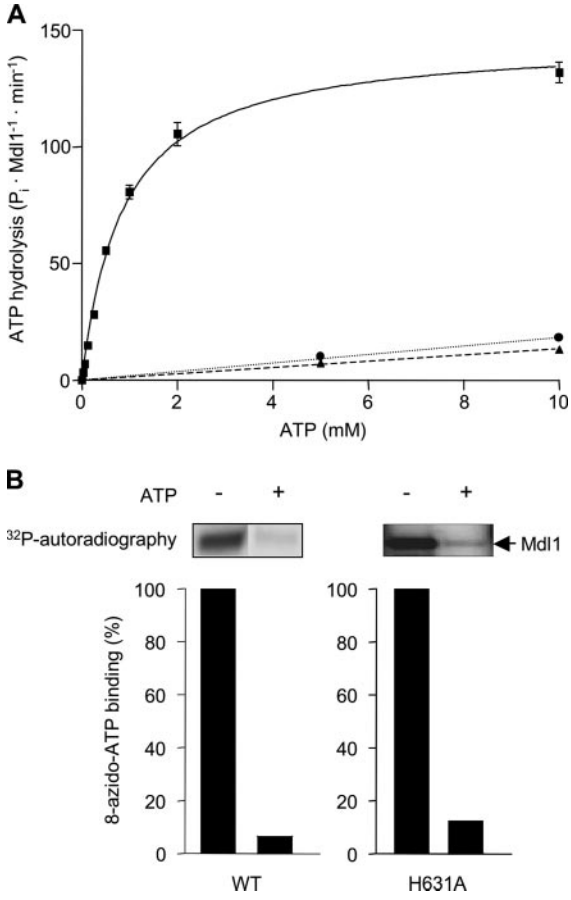

FIGURE 4. **ATPase activity of wild-type and mutant Mdl1.** *A*, the ATPase activity of Mdl1 (0.1 μM) was measured as a function of the ATP concentration at 30 °C. Digitonin-solubilized wild-type Mdl1 (*squares*) is active in ATP hydrolysis with a k_{cat} of 2.6 ATP per second and a K_m of 0.86 mM. The data were fitted to the Hill equation $y = (ax^n/(b^n + x^n))$, resulting in a best fit ($R^2 = 0.98$) with a Hill coefficient (n) of 0.98. The H631A (*triangles*) and E599Q mutant (*circles*) showed only background ATPase activity. *B*, the H631A mutant bound ATP as wild-type (*WT*) Mdl1 as shown by 8-azido-[α-^{32}P]ATP photo cross-linking. The experiments were performed as described in Fig. 3. The photo cross-linking can be blocked by an excess of MgATP (3 mM).

tern (inhibition from 85 to 50%; Fig. 3*C*) as observed for the isolated NBD (22). AMP-PNP bound with a reduced affinity, demonstrating previous observations that AMP-PNP does not perfectly mimic ATP. As expected, AMP did not compete for 8-azido-ATP binding. Taken together, these results show that full-length Mdl1 has a nucleotide specificity similar to that of the isolated NBD (22).

We next analyzed the ATPase activity of the digitonin-solubilized Mdl1. The ATP hydrolysis showed Michaelis-Menten kinetics (Hill coefficient of 0.98) with a $K_{m(ATP)}$ of 0.86 ± 0.06 mM, a V_{max} of 2.3 μmol·min^{-1}·mg^{-1}, and a turnover rate (k_{cat}) of 2.6 ± 0.1 ATP/s (per Mdl1 subunit) (Fig. 4*A*). To confirm that the ATPase activity was Mdl1-specific and not from a co-purified, highly active ATPase, Mdl1 mutants were analyzed, solubilized, and purified identically to the wild type. Mutation of the putative catalytic base (E599Q) or the histidine in the H-loop (H631A) resulted in background ATPase activity (Fig. 4*A*). Notably, the ATP binding properties of both mutants remained preserved as compared with wild type (Fig. 4*B*; E599Q not shown). Strikingly, the ATPase activity of full-length Mdl1 is at least 2

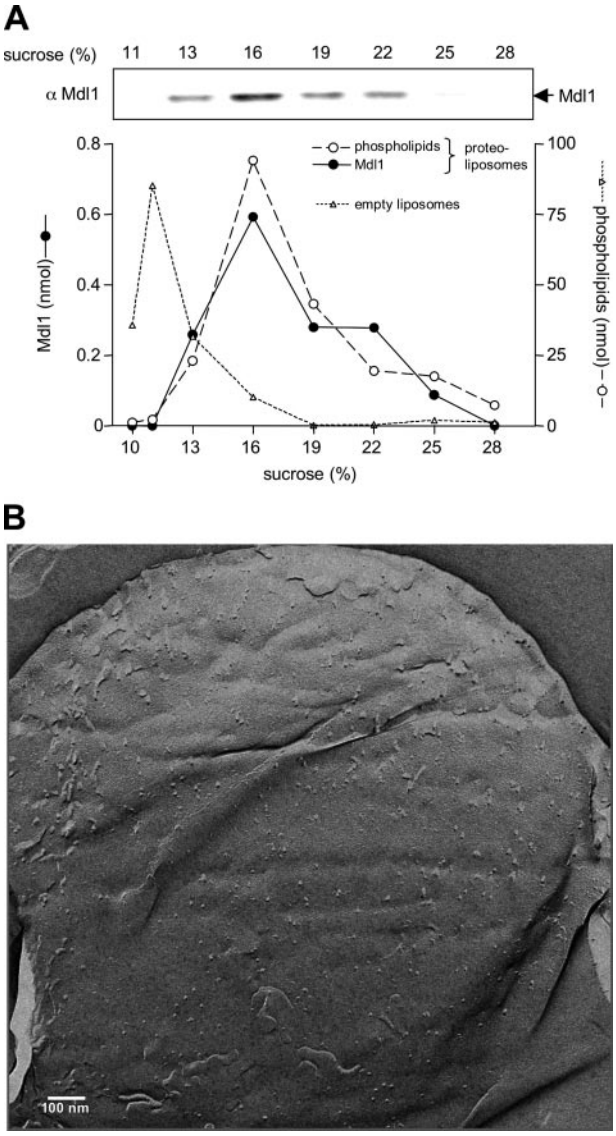

FIGURE 5. **Reconstitution of Mdl1.** *A*, empty or Mdl1-containing liposomes were applied to a sucrose gradient centrifugation. The fractions were analyzed with respect to the amount of Mdl1 and phospholipids. Reconstitution was evident from co-migration of the lipid and Mdl1 fraction (16% sucrose). A molar phospholipid-to-Mdl1 ratio of 160 was determined. Empty liposomes migrate at 11% sucrose. *B*, proteoliposomes were analyzed by freeze fracture electron microscopy. A statistical analysis revealed a homogenous particle size distribution of 10 ± 2 nm in diameter.

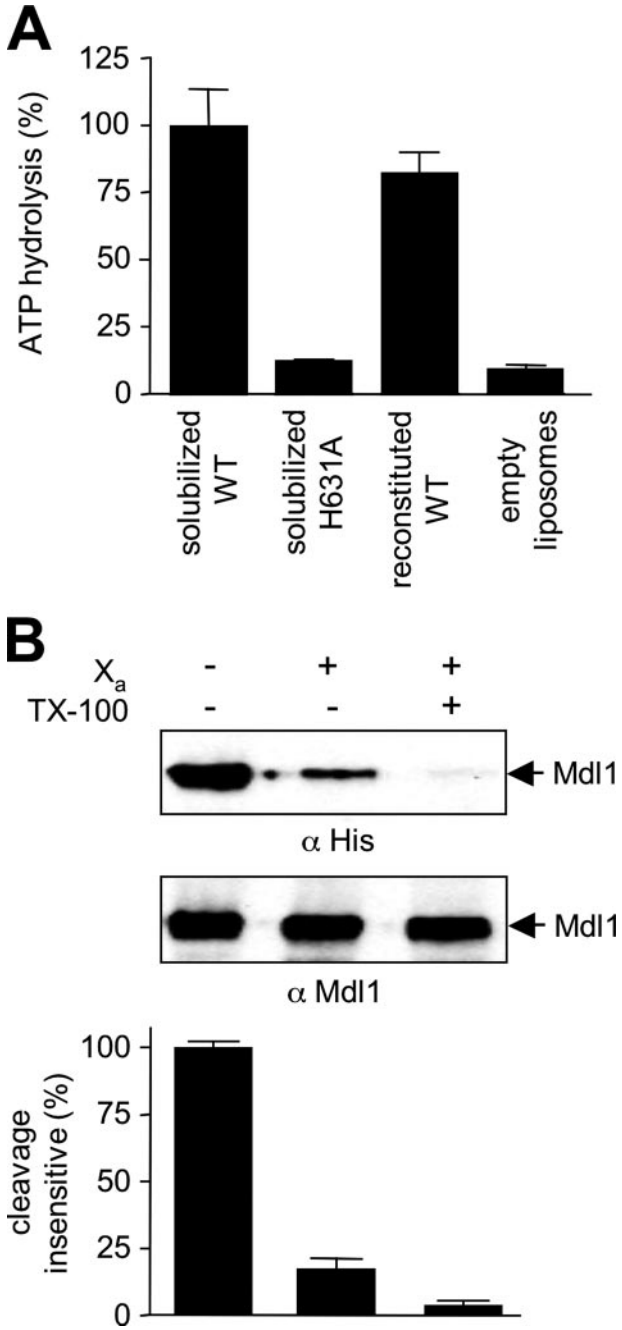

FIGURE 6. **ATPase activity and orientation of reconstituted Mdl1.** *A*, the ATPase activity of reconstituted Mdl1 was measured for 10 min at 30 °C in presence of 5 mM MgATP. After reconstitution, 85% of the activity of the digitonin-solubilized Mdl1 (wild type) was recovered. The H631A mutant is shown as control. *B*, the orientation of reconstituted Mdl1 was determined by protease protection assays utilizing the X_a cleavage site at the C terminus of Mdl1. Mdl1-containing liposomes were incubated with factor X_a (10 μg/ml) for 2 h at 25 °C in buffer R containing 1 mM $CaCl_2$. Cleavage of the C-terminal His_8 tag and thus orientation of Mdl1 was followed by an anti-His antibody. 20 ± 5% of reconstituted Mdl1 remain uncleaved, demonstrating that 80% of the NBDs are in an outside orientation. Triton X-100 (2%) was used to permeabilize the proteoliposomes (almost 100% cleavage). The data are derived from three independent measurements. The anti-Mdl1 antibody was used as loading control. *WT*, wild type; *TX-100*, Triton X-100.

orders of magnitude higher than observed for the isolated NBD (43). Furthermore, the turnover rate of full-length Mdl1 is constant over a large concentration range (0.01–1 μM) in contrast to the isolated NBD, which is nonlinearly dependent on the NBD concentration.

To analyze the mitochondrial ABC transporter in its membrane-embedded state, Mdl1 was reconstituted into liposomes. Purified Mdl1 was mixed with DDM-destabilized liposomes composed of *E. coli* lipids. Subsequently, the detergent was removed by absorption to Bio-beads. Protein reconstitution was analyzed by sucrose gradient centrifugation. Reconstitution of Mdl1 into the liposomes is evident from the co-migration of protein and lipids (Fig. 5*A*). Mdl1-containing liposomes were recovered at 16% sucrose, whereas empty liposomes migrated at 11% sucrose. No protein was detected at the bottom of the gradient, indicating that Mdl1 did not precipitate and thus was efficiently inserted into liposomes. As demonstrated by freeze fracture electron microscopy, well formed lipid vesi-

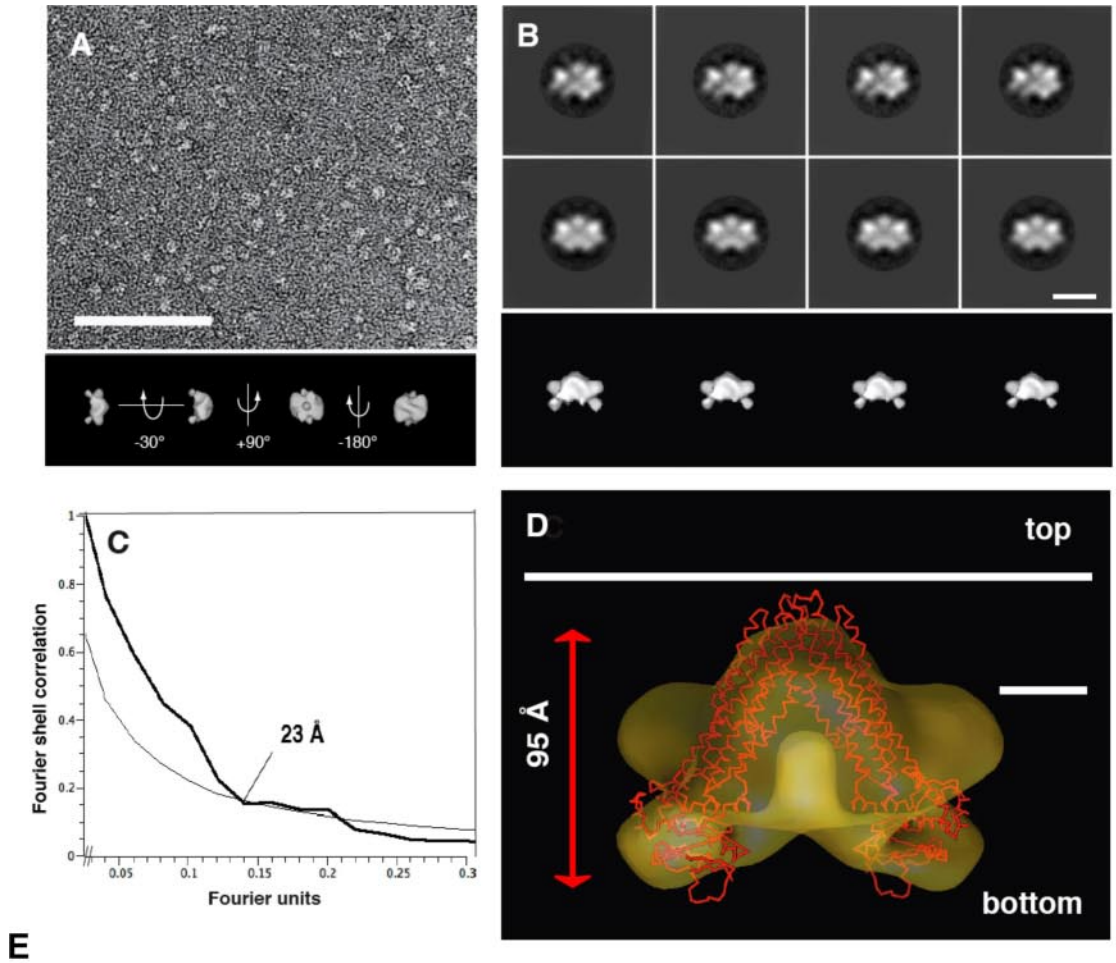
A
B
-30°
+90°
-180°
C
Fourier shell correlation
23 Å
Fourier units
D
top
95 Å
bottom

E

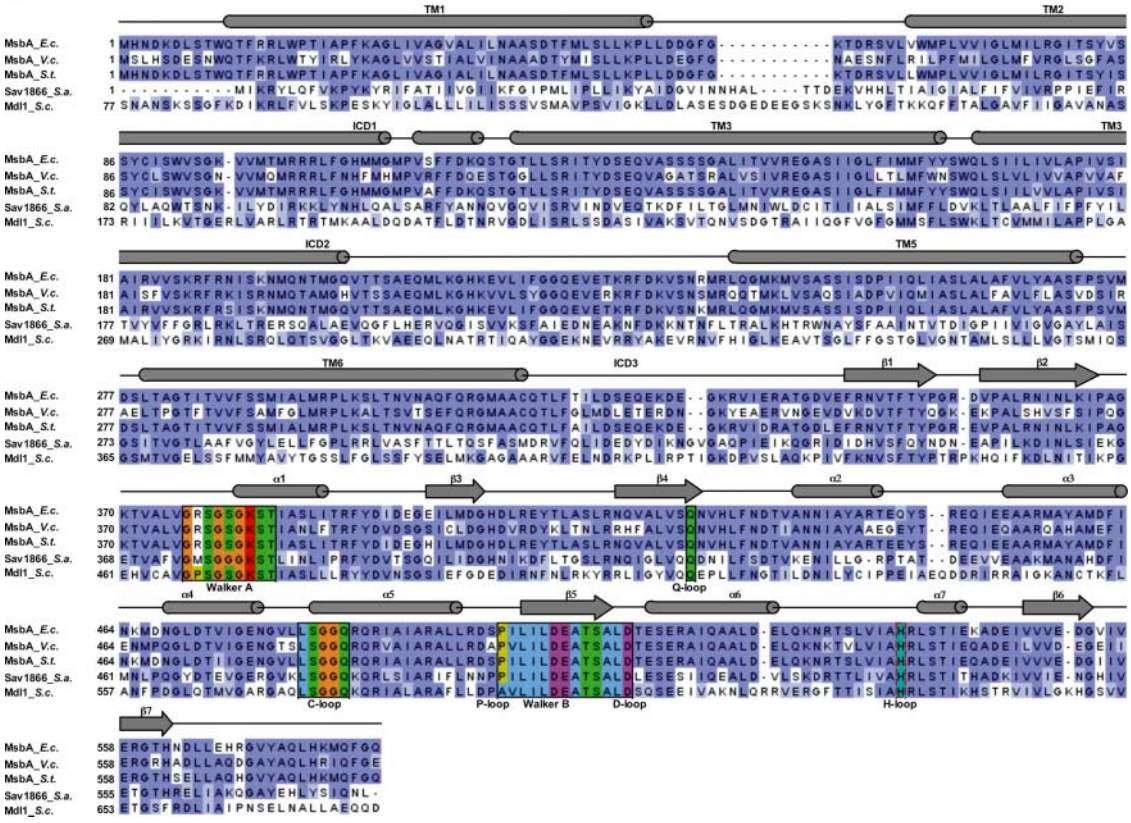
TM1
TM2
ICD1
TM3
TM3
ICD2
TM5
TM6
ICD3
β1
β2
α1
β3
β4
α2
α3
Walker A
α4
α5
β5
Q-loop
α6
α7
β6
C-loop
P-loop
Walker B
D-loop
H-loop
β7
MsbA_E.c.
MsbA_V.c.
MsbA_S.t.
Sav1866_S.a.
Mdl1_S.c.

cles with incorporated protein particles are formed (Fig. 5*B*). A statistic analysis revealed that the diameter of the particles is homogeneous and roughly 10 ± 2 nm. Analysis of the protein and lipid content of the proteoliposomes demonstrated that Mdl1 was reconstituted at a molar lipid-to-protein ratio of 160. We next investigated the ATPase activity of Mdl1 embedded in membranes. Remarkably, 85% of the ATPase activity of the solubilized protein was recovered (Fig. 6*A*). Taking advantage of the factor X_a cleavage site in front of the C-terminal His_8 tag, protease protection assays revealed that 80 ± 5% of Mdl1 are reconstituted in an "NBD-out" orientation (Fig. 6*B*). In the range of error, this result is consistent with the 85% ATPase activity of solubilized Mdl1, demonstrating that solubilized and reconstituted Mdl1 have a similar ATPase activity.

Mdl1 was proposed to be involved in the peptide export from the mitochondrial matrix (5). However, direct transport assays have not been performed so far. Combinatorial peptide libraries were instrumental to decipher the substrate specificity of ABC transporters (44–47). We therefore examined peptide uptake in the reconstituted system by using radiolabeled peptide libraries, X_8 and X_{23}, where *X* represents all 19 genetically encoded amino acids except cysteine in equimolar distribution. To our surprise, in extensive studies we did not detect an Mdl1-dependent peptide transport activity into the liposomes. In addition, no peptide-stimulated ATPase activity of Mdl1 was observed (data not shown). We thus conclude that Mdl1, if indeed it functions as a peptide transporter, recognizes a very specific subset of peptides or specifically modified peptides and is therefore distinct from other peptide transporters such as transporter associated with antigen processing (TAP), TAP-like, or OppA (44–47).

The random-conical tilt reconstruction method, particularly suitable for generating first three-dimensional maps of yet unknown protein complexes, was chosen to investigate the quarternary structure of several ABC transporters (48–53). The structure of digitonin-solubilized Mdl1 particles was investigated by single-particle analysis. Fig. 7*A* shows a representative micrograph of Mdl1 particles after negative staining. The image depicts particles of a size range expected for the molecular mass determined by size exclusion chromatography and Blue native electrophoresis. Importantly, a mock isolation and purification from mitochondria without induced expression of recombinant Mdl1 did not reveal particles of that kind and size.

Equivalent particles were selected from several pairs of micrographs (2 × 1,404 particles; tilted and untilted of the same area). Particles from the zero degree images were translationally and rotationally aligned to one reference and subsequently analyzed using the neural network approach (32). After several multireference alignments with an increasing number of references, final class averages like in Fig. 7*B* (*first row*) were obtained, representing >50% of the data set. Four to six prominent stain-excluding densities are connected via stain-filled extensions showing the preferred orientation on the carbon support film. They appear to be almost symmetric when compared with the corresponding symmetrized class averages (Fig. 7*B*, *second row*), consistent with the biochemical evidence of homodimeric Mdl1.

A three-dimensional volume at a final resolution of 23 Å (FSC_5; Fig. 7*C*) was calculated from corresponding tilted particles. 2-Fold symmetry in the direction of the *z* axis and perpendicular to the membrane plane was enforced at the latest step (Fig. 7, *A*, *lower panel*; *B*, *third row*; and *D*). The dimensions of the volume were determined to 125 × 110 × 95 $Å^3$. Again, the four density lobes found in prominent views with the *z* direction in the paper plane are easily recognizable independent of the surface threshold level (Fig. 7*B*, *third row*). Moreover, a V-shaped outline of the electron density surface pointed to a homodimeric state of Mdl1.

To investigate these findings in more detail, several MsbA-like proteins with solved crystal structures were compared with the calculated electron density map of Mdl1 (34, 54–56). A sequence alignment of MsbA from *E. coli*, *Vibrio cholera*, and *Salmonella typhimurium*, Sav1866 from *Staphylococcus aureus*, and Mdl1 from *S. cerevisiae* demonstrates their high similarity (51%; Fig. 7*E*). Interestingly, it was found that exclusively the open form of *E. coli* MsbA fitted exactly in terms of dimensions and space (Fig. 7*D*). The potential nucleotide-binding domains appear to be separated by more than 50 Å (Fig. 7*D*, *bottom*). We therefore conclude that our reconstruction reveals a homodimeric Mdl1 complex in an open conformation with the NBDs clearly separated.

DISCUSSION

Mitochondrial ABC transporters are difficult to study because of the two-membrane architecture of mitochondria, problems associated with analyzing an export process, and the high abundance of other ATPases and carriers/transporters. This asks for an *in vitro* system with pure and active protein. By systematic screens, we have established the overexpression of Mdl1 and present the first functional and structural analysis of a mitochondrial ABC transporter. Driven by an inducible promotor from a multicopy plasmid, a 100-fold overexpression of Mdl1 was achieved in *S. cerevisiae*. After screening optimal conditions for solubilization, the transporter was purified to homogeneity via metal affinity chromatography. The functional properties of solubilized as well as membrane-reconsti-

FIGURE 7. **Single particle electron microscopy of Mdl1.** *A*, *upper panel*, representative electron micrograph of negatively stained single Mdl1 complexes. *Scale bar*, 100 nm. *Lower panel*, different views of the final reconstruction (2-fold symmetrized). Rotational transitions are defined by *arrows* and corresponding angles. *B*, *first row*, representative class averages (>50% of the data set) obtained after multireference alignments showing the preferred orientation. The imaginary *z* direction is parallel to the paper plane. *Second row*, corresponding symmetrized class averages *Scale bar*, 100 Å. *Third row*, corresponding surface view of the reconstruction with increasing threshold levels from *left* to *right*. *C*, resolution of the final three-dimensional reconstruction at 23 Å. Fourier shell correlation curve (*thick solid line*) and the five sigma threshold (*thin solid line*) are shown. *D*, comparison of Mdl1 and the crystal structure of the V-shaped MsbA-dimer from *E. coli*. The homodimer of MsbA (Protein Data Bank code 1JSQ, in *red*) was fitted into the three-dimensional electron density map of Mdl1 depicted as translucent isosurface in *yellow*. *White horizontal lines* indicate the dimension of a membrane. The *z* axis is parallel to the scale bar and perpendicular to the membrane plane. *E*, sequence alignment of MsbA from *E. coli*, *V. cholera*, and *S. typhimurium* (Protein Data Bank codes 1JSQ, open form (34); 1PF4, closed form (54); and 1Z2R, closed form (55)), Sav1866 from *S. aureus* (2HYD (56)), and Mdl1 (gi 6323217). The Walker A and B motifs, the Q-, C-, P-, D-, and H-loops are *boxed* and colored according to chemical properties of the amino acid residues. The overall color code results from the BLOSUM62 score.

tuted Mdl1 in respect to ATP binding and ATP hydrolysis were characterized in detail. Finally, a first three-dimensional map of the mitochondrial ABC transporter was obtained by single particle EM analysis.

The choice of the detergent used for the solubilization and purification of Mdl1 turned out to be critical. First, reasonable amounts of Mdl1 must be extracted from the membrane, which is best achieved by FC-14, and second, the oligomeric state and activity of the protein must be preserved. After purification in digitonin, Mdl1 was found to be mostly monodisperse by Blue native electrophoresis and showed the highest ATPase activity ($V_{max} = 2.3\ \mu mol \cdot min^{-1} \cdot mg^{-1}$). The observed activity is higher than reported for the majority of ABC transporters, *e.g.* MRP ($0.46\ \mu mol \cdot min^{-1} \cdot mg^{-1}$), MsbA ($0.04-0.15\ \mu mol \cdot min^{-1} \cdot mg^{-1}$), or BmrA ($1.2\ \mu mol \cdot min^{-1} \cdot mg^{-1}$) (57–59). Only Atm1 showed a similar ATPase turnover number of $127\ min^{-1}$ ($V_{max} = 1.9\ \mu mol \cdot min^{-1} \cdot mg^{-1}$) compared with $156\ min^{-1}$ in case of Mdl1 (60). The high ATPase activity indicates that solubilized Mdl1 is in an active state. This conclusion is further supported by the observation that solubilized and reconstituted Mdl1 have a similar ATPase activity.

Mdl1 binds MgATP with a remarkably high affinity ($K_d = 0.26\ \mu M$) in comparison with the isolated NBD ($K_d = 2\ \mu M$) (22). This value is also 2 orders of magnitude lower as compared with other ABC transporters (44, 61–63). Moreover, the apparent affinity for MgATP is 3,000 times higher than the Michaelis-Menten constant for ATP hydrolysis ($K_{m(ATP)} = 0.86\ mM$). This implies that ATP binding and ATP hydrolysis are distinct steps. Remarkably, the activity of the isolated NBD is strongly dependent on the NBD concentration, whereas the ATP turnover of the full-length Mdl1 is concentration-independent (not shown). This demonstrates that in the full-length complex, the association rate of the NBDs (dimer formation) is not rate-limiting for ATP hydrolysis because of the close proximity and high local concentration within the transport complex.

Although Mdl1 is highly active in ATP hydrolysis, we did not observe a peptide-stimulated ATPase nor a peptide transport activity. We propose that this is either due to the fact that Mdl1 recognizes a very specific subset of peptides, which is underrepresented in the peptide libraries, or that the substrate of Mdl1 is more complex than originally anticipated, including modifications or associated cofactors. These findings challenge the initial observation that Mdl1 functions as peptide exporter in mitochondrial quality control (5). As was found to be case for Atm1, extensive screens will be required to resolve the issue of substrate specificity of Mdl1.

In this work, a first three-dimensional map of homodimeric Mdl1 complex has been determined by electron microscopy and single particle analysis. Single-particle analysis has successfully been applied to other ABC transporters, demonstrating the power of this method for particles even below 0.5 MDa. The Mdl1 preparation method uses digitonin to extract the protein from the membrane, metal affinity purification, and gel filtration. This procedure yields monodisperse Mdl1 particles suitable for structure determination.

Mdl1 appears to be in a homodimeric state because the dimensions of the particle of $125 \times 110 \times 95\ Å^3$ are too small for a dimer of a dimer and too large for a monomer. This conclusion is consistent with data derived from Blue native electrophoresis, gel filtration, and the diameter of membrane-embedded Mdl1 particles (freeze fracture EM). Remarkably, reconstructions obtained for different ABC transporters so far have been interpreted diversely in terms of their oligomerization state. The full size transporters PDR5 (63) and CFTR (61) showed particle dimensions that fit (homo) dimers, whereas for particles of the full size transporter P-glycoprotein a monomeric state was consistent (64). Dimensions of the half-size transport complex TAP1/TAP2 and YvcC implicate heterodimeric or homodimeric structures, respectively (49, 53).

The Mdl1 structure is clearly different from the very recently solved x-ray structure of the ABC transporter Sav1866 from *S. aureus*, which is found in an outward facing conformation with the two NBDs in close contact (56). Taken together, this analysis provides the first three-dimensional map of a mitochondrial ABC transporter. The outline and overall dimensions of the reconstruction as well as its 2-fold symmetry indicate that the Mdl1 complex is formed by a homodimer in the open conformation. Comparison with ABC transporters operating as exporters suggests major differences in the organization of the transmembrane domains within the transport cycle. However, x-ray and EM structures represent snapshots of different states, and the different overall organization of the TMDs and arrangement of transmembrane helices indicate very small energy barriers between these forms. This may allow for accommodating a broad spectrum of transported substrates. The high ATPase activity compared with other ABC transporters as well as the preserved homooligomeric state of MDL1 suggest that the open EM structure represents an active conformation within the catalytic cycle and not an inactive, stable state. Furthermore, detergent artifacts disrupting the oligomeric complex and thereby forming new packing contacts of the TMDs can be excluded. Based on this structural information on MDL1 at low resolution, it would be highly eligible to obtain a high resolution structure of an ABC exporter, such as Sav1866, in an open inward facing conformation. The overexpression and straightforward purification of Mdl1 provide the basis for future studies on the structure and function of Mdl1.

Acknowledgments—We thank Tobias Beckhaus and Heidi Betz for technical assistances. We thank Drs. Rupert Abele, Joachim Koch, Lutz Schmitt, and David Parcej for helpful discussions.

REFERENCES

1. Higgins, C. F. (1992) *Annu. Rev. Cell Biol.* **8,** 67–113
2. Davidson, A. L., and Chen, J. (2004) *Annu. Rev. Biochem.* **73,** 241–268
3. van der Does, C., and Tampé, R. (2004) *Biol. Chem.* **385,** 927–933
4. Dean, M., Allikmets, R., Gerrard, B., Stewart, C., Kistler, A., Shafer, B., Michaelis, S., and Strathern, J. (1994) *Yeast* **10,** 377–383
5. Young, L., Leonhard, K., Tatsuta, T., Trowsdale, J., and Langer, T. (2001) *Science* **291,** 2135–2138
6. Arnold, I., and Langer, T. (2002) *Biochim. Biophys. Acta* **1592,** 89–96
7. Hogue, D. L., Liu, L., and Ling, V. (1999) *J. Mol. Biol.* **285,** 379–389
8. Shirihai, O. S., Gregory, T., Yu, C., Orkin, S. H., and Weiss, M. J. (2000) *EMBO J.* **19,** 2492–2502
9. Zhang, F., Hogue, D. L., Liu, L., Fisher, C. L., Hui, D., Childs, S., and Ling, V. (2000) *FEBS Lett.* **478,** 89–94
10. Chloupkova, M., LeBard, L. S., and Koeller, D. M. (2003) *J. Mol. Biol.* **331,**

155–165
11. Kispal, G., Csere, P., Prohl, C., and Lill, R. (1999) *EMBO J.* **18,** 3981–3989
12. Uebel, S., Meyer, T. H., Kraas, W., Kienle, S., Jung, G., Wiesmüller, K. H., and Tampé, R. (1995) *J. Biol. Chem.* **270,** 18512–18516
13. van der Sluis, E. O., Nouwen, N., and Driessen, A. J. (2002) *FEBS Lett.* **527,** 159–165
14. Wach, A., Brachat, A., Pohlmann, R., and Philippsen, P. (1994) *Yeast* **10,** 1793–1808
15. Wolfger, H., Mahe, Y., Parle-McDermott, A., Delahodde, A., and Kuchler, K. (1997) *FEBS Lett.* **418,** 269–274
16. Miroux, B., and Walker, J. E. (1996) *J. Mol. Biol.* **260,** 289–298
17. Baneyx, F., and Georgiou, G. (1990) *J. Bacteriol.* **172,** 491–494
18. Jobling, M. G., and Holmes, R. K. (1990) *Nucleic Acids Res.* **18,** 5315–5316
19. van der Laan, M., Houben, E. N., Nouwen, N., Luirink, J., and Driessen, A. J. (2001) *EMBO Rep.* **2,** 519–523
20. de Ruyter, P. G., Kuipers, O. P., and de Vos, W. M. (1996) *Appl. Environ. Microbiol.* **62,** 3662–3667
21. van der Does, C., de Keyzer, J., van der Laan, M., and Driessen, A. J. (2003) *Methods Enzymol.* **372,** 86–98
22. Janas, E., Hofacker, M., Chen, M., Gompf, S., van der Does, C., and Tampé, R. (2003) *J. Biol. Chem.* **278,** 26862–26869
23. Brachmann, C. B., Davies, A., Cost, G. J., Caputo, E., Li, J., Hieter, P., and Boeke, J. D. (1998) *Yeast* **14,** 115–132
24. Sherman, F. (1991) *Methods Enzymol.* **194,** 3–21
25. Meisinger, C., Sommer, T., and Pfanner, N. (2000) *Anal. Biochem.* **287,** 339–342
26. Schagger, H. (2001) *Methods Cell Biol.* **65,** 231–244
27. Cheng, Y., and Prusoff, W. H. (1973) *Biochem. Pharmacol.* **22,** 3099–3108
28. Gorbulev, S., Abele, R., and Tampé, R. (2001) *Proc. Natl. Acad. Sci. U. S. A.* **98,** 3732–3737
29. Chen, P. S., Toribara, T. Y., and Warner, H. (1956) *Anal. Chem.* **28,** 1756–1758
30. Chen, M., Abele, R., and Tampé, R. (2003) *J. Biol. Chem.* **278,** 29686–29692
31. Frank, J., Radermacher, M., Penczek, P., Zhu, J., Li, Y., Ladjadj, M., and Leith, A. (1996) *J. Struct. Biol.* **116,** 190–199
32. Sorzano, C. O., Marabini, R., Velazquez-Muriel, J., Bilbao-Castro, J. R., Scheres, S. H., Carazo, J. M., and Pascual-Montano, A. (2004) *J. Struct. Biol.* **148,** 194–204
33. Radermacher, M., Wagenknecht, T., Verschoor, A., and Frank, J. (1987) *J. Microsc.* **146,** 113–136
34. Chang, G., and Roth, C. B. (2001) *Science* **293,** 1793–1800
35. Pettersen, E. F., Goddard, T. D., Huang, C. C., Couch, G. S., Greenblatt, D. M., Meng, E. C., and Ferrin, T. E. (2004) *J. Comput. Chem.* **25,** 1605–1612
36. Ghaemmaghami, S., Huh, W. K., Bower, K., Howson, R. W., Belle, A., Dephoure, N., O'Shea, E. K., and Weissman, J. S. (2003) *Nature* **425,** 737–741
37. Kunji, E. R., Slotboom, D. J., and Poolman, B. (2003) *Biochim. Biophys. Acta* **1610,** 97–108
38. Meyers, S., Schauer, W., Balzi, E., Wagner, M., Goffeau, A., and Golin, J. (1992) *Curr. Genet* **21,** 431–436
39. Wada, S., Niimi, M., Niimi, K., Holmes, A. R., Monk, B. C., Cannon, R. D., and Uehara, Y. (2002) *J. Biol. Chem.* **277,** 46809–46821
40. Decottignies, A., Grant, A. M., Nichols, J. W., de Wet, H., McIntosh, D. B., and Goffeau, A. (1998) *J. Biol. Chem.* **273,** 12612–12622
41. Margolles, A., Putman, M., van Veen, H. W., and Konings, W. N. (1999) *Biochemistry* **38,** 16298–16306
42. Schägger, H., and Pfeiffer, K. (2000) *EMBO J.* **19,** 1777–1783
43. van der Does, C., Presenti, C., Schulze, K., Dinkelaker, S., and Tampé, R. (2006) *J. Biol. Chem.* **281,** 5694–5701
44. Wolters, J. C., Abele, R., and Tampé, R. (2005) *J. Biol. Chem.* **280,** 23631–23636
45. Uebel, S., Kraas, W., Kienle, S., Wiesmüller, K. H., Jung, G., and Tampé, R. (1997) *Proc. Natl. Acad. Sci. U. S. A.* **94,** 8976–8981
46. Detmers, F. J., Lanfermeijer, F. C., Abele, R., Jack, R. W., Tampé, R., Konings, W. N., and Poolman, B. (2000) *Proc. Natl. Acad. Sci. U. S. A.* **97,** 12487–12492
47. Doeven, M. K., Abele, R., Tampé, R., and Poolman, B. (2004) *J. Biol. Chem.* **279,** 32301–32307
48. Awayn, N. H., Rosenberg, M. F., Kamis, A. B., Aleksandrov, L. A., Riordan, J. R., and Ford, R. C. (2005) *Biochem. Soc. Trans.* **33,** 996–999
49. Chami, M., Steinfels, E., Orelle, C., Jault, J. M., Di Pietro, A., Rigaud, J. L., and Marco, S. (2002) *J. Mol. Biol.* **315,** 1075–1085
50. Ferreira-Pereira, A., Marco, S., Decottignies, A., Nader, J., Goffeau, A., and Rigaud, J. L. (2003) *J. Biol. Chem.* **278,** 11995–11999
51. Rosenberg, M. F., Callaghan, R., Ford, R. C., and Higgins, C. F. (1997) *J. Biol. Chem.* **272,** 10685–10694
52. Rosenberg, M. F., Mao, Q., Holzenburg, A., Ford, R. C., Deeley, R. G., and Cole, S. P. (2001) *J. Biol. Chem.* **276,** 16076–16082
53. Velarde, G., Ford, R. C., Rosenberg, M. F., and Powis, S. J. (2001) *J. Biol. Chem.* **276,** 46054–46063
54. Chang, G. (2003) *J. Mol. Biol.* **330,** 419–430
55. Reyes, C. L., and Chang, G. (2005) *Science* **308,** 1028–1031
56. Dawson, R. J., and Locher, K. P. (2006) *Nature* **443,** 180–185
57. Ravaud, S., Do Cao, M. A., Jidenko, M., Ebel, C., Le Maire, M., Jault, J. M., Di Pietro, A., Haser, R., and Aghajari, N. (2006) *Biochem. J.* **395,** 345–353
58. Doerrler, W. T., and Raetz, C. R. (2002) *J. Biol. Chem.* **277,** 36697–36705
59. Chang, X. B., Hou, Y. X., and Riordan, J. R. (1997) *J. Biol. Chem.* **272,** 30962–30968
60. Kuhnke, G., Neumann, K., Muhlenhoff, U., and Lill, R. (2006) *Mol. Membr. Biol.* **23,** 173–184
61. Horn, C., Bremer, E., and Schmitt, L. (2003) *J. Mol. Biol.* **334,** 403–419
62. Lapinski, P. E., Raghuraman, G., and Raghavan, M. (2003) *J. Biol. Chem.* **278,** 8229–8237
63. Qu, Q., Russell, P. L., and Sharom, F. J. (2003) *Biochemistry* **42,** 1170–1177
64. van der Does, C., Manting, E. H., Kaufmann, A., Lutz, M., and Driessen, A. J. (1998) *Biochemistry* **37,** 201–210